

IL-6 trans-signaling promotes pancreatitis-associated lung injury and lethality

Hong Zhang,¹ Patrick Neuhöfer,¹ Liang Song,¹ Björn Rabe,² Marina Lesina,¹ Magdalena U. Kurkowski,¹ Matthias Treiber,¹ Thomas Wartmann,³ Sara Regnér,⁴ Henrik Thorlacius,⁴ Dieter Saur,¹ Gregor Weirich,⁵ Akihiko Yoshimura,⁶ Walter Halangk,³ Joseph P. Mizgerd,⁷ Roland M. Schmid,¹ Stefan Rose-John,² and Hana Algül¹

¹II. Medizinische Klinik, Klinikum rechts der Isar, Technische Universität München, Munich, Germany. ²Institute of Biochemistry, Christian-Albrechts-University of Kiel, Kiel, Germany. ³Department of Surgery, Division of Experimental Surgery, Otto-von-Guericke University, Magdeburg, Germany. ⁴Department of Clinical Sciences, Malmö, Section for Surgery, Lund University, Malmö, Sweden. ⁵Pathologisches Institut, Klinikum rechts der Isar der Technischen Universität München, Munich, Germany. ⁶Department of Microbiology and Immunology, Keio University School of Tokyo, and Japan Science and Technology Agency (JST), CREST, Chiyoda-ku, Tokyo, Japan. ⁷Pulmonary Center, Boston University School of Medicine, Boston, Massachusetts, USA.

Acute lung injury (ALI) is an inflammatory disease with a high mortality rate. Although typically seen in individuals with sepsis, ALI is also a major complication in severe acute pancreatitis (SAP). The pathophysiology of SAP-associated ALI is poorly understood, but elevated serum levels of IL-6 is a reliable marker for disease severity. Here, we used a mouse model of acute pancreatitis-associated (AP-associated) ALI to determine the role of IL-6 in ALI lethality. *Il6*-deficient mice had a lower death rate compared with wild-type mice with AP, while mice injected with IL-6 were more likely to develop lethal ALI. We found that inflammation-associated NF- κ B induced myeloid cell secretion of IL-6, and the effects of secreted IL-6 were mediated by complexation with soluble IL-6 receptor, a process known as trans-signaling. IL-6 trans-signaling stimulated phosphorylation of STAT3 and production of the neutrophil attractant CXCL1 in pancreatic acinar cells. Examination of human samples revealed expression of IL-6 in combination with soluble IL-6 receptor was a reliable predictor of ALI in SAP. These results demonstrate that IL-6 trans-signaling is an essential mediator of ALI in SAP across species and suggest that therapeutic inhibition of IL-6 may prevent SAP-associated ALI.

Introduction

Acute pancreatitis (AP) accounts for more than 220,000 hospital admissions in the United States each year. Risk factors for AP include gallstones and excessive alcohol use. Interestingly, 70%–80% of AP patients develop mild and uncomplicated AP, while 20%–30% will develop more severe symptoms with concomitant multiple organ failure (MOF) (1). MOF is a consequence of the systemic activation of the immune system, known as systemic inflammatory response syndrome (SIRS). The clinical and pathological features of SIRS mimic those of sepsis; however, efforts to identify any infecting organisms in many patients with SIRS have failed (2–4). Although this syndrome is typically seen in individuals with sepsis, SIRS also occurs in patients with severe AP (SAP), blunt trauma, aseptic burns, and widespread surgical manipulations (5, 6). A major complication during SAP is acute lung injury (ALI). Nevertheless, the clinical course of ALI in SAP is still unpredictable and has a mortality rate of up to 50%. Current therapeutic approaches in SAP and associated ALI are symptomatically based (1, 7).

The pathophysiology of SAP with ALI is poorly understood. Researchers have long hypothesized that SAP results from activation of digestive enzymes within the pancreas, a process called autodigestion (8). Indeed, inherited mutations in genes encoding for digestive enzymes have been found in patients with a hereditary form of pancreatitis. However, all these patients develop chronic pancreatitis, rather than SAP with ALI (9, 10). Therefore,

in recent years, a novel concept evolved suggesting that systemic complications during AP result from uncontrolled activation of the immune system (5). In an attempt to identify surrogate parameters as predictors for complicated AP, several association studies linking cytokines and chemokines with AP severity have been conducted (11). Among these, serum levels of IL-6 and the IL-6-dependent acute phase protein C-reactive protein (CRP) were identified as the most reliable parameters for SAP (12, 13). Research has yet to establish whether IL-6 or CRP are merely markers or have any pathophysiological impact.

IL-6 and CRP are known to be involved in the STAT3/SOCS3 cascade (14). Belonging to the family of gp130 ligands (including leukemia inhibitory factor [LIF], oncostatin M [OSM], cardiotrophin-like cytokine [CLC], ciliary neurotrophic factor [CNTF], IL-11, and IL-27), IL-6 transmits signals by binding to its membrane-bound receptor, IL-6R, and the ubiquitously expressed gp130 receptor. 2 distinct processes control IL-6 responses in vivo. IL-6 signals are mediated via gp130 either through IL-6 engagement of IL-6R or through complexation with soluble IL-6R (sIL-6R), which is termed IL-6 trans-signaling (15–17). Because IL-6R is only minimally expressed (mainly on hepatocytes and leukocytes), IL-6 trans-signaling dramatically increases the number of potential IL-6 target cells (16). The complexes involve the downstream kinase Jak-2 in order to phosphorylate the transcription factor STAT3 at Y705 (18, 19). Tyrosine phosphorylation of Y705 is required for formation of homodimers and subsequent nuclear translocations. STAT3 is involved in regulation of apoptosis, angiogenesis, inflammation, and acute phase response, including CRP expression in hepatocytes. Termination of STAT3 signaling is mediated by the endogenous inhibitor SOCS3 (20).

Authorship note: Hong Zhang and Patrick Neuhöfer contributed equally to this work.

Conflict of interest: Stefan Rose-John is an inventor of patents that describe the function of sgp130Fc and is a shareholder of the Conaris Research Institute.

Citation for this article: *J Clin Invest.* 2013;123(3):1019–1031. doi:10.1172/JCI64931.

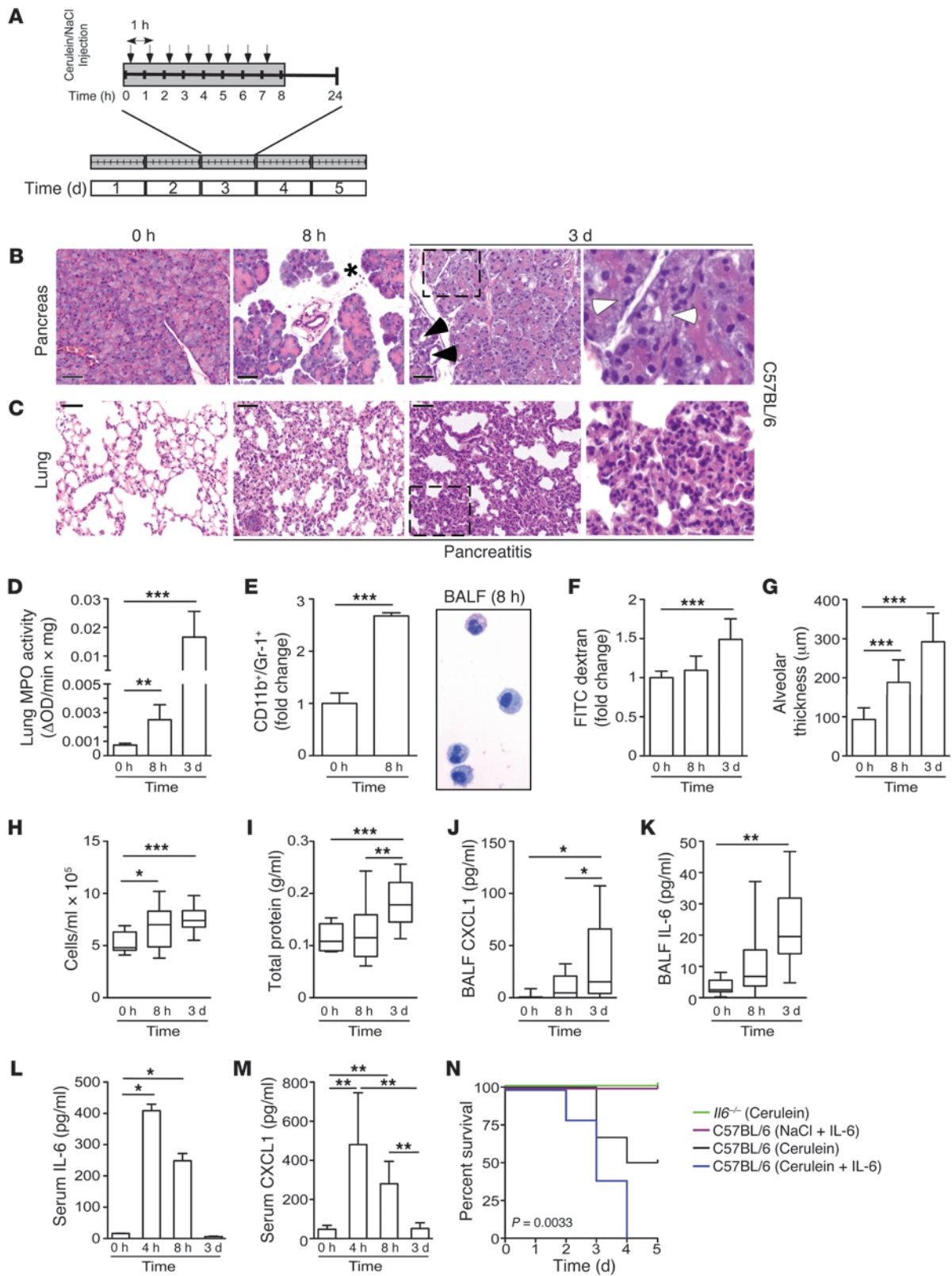




Figure 1

IL-6 levels correlate with the extent of pulmonary damage and lethality during SAP. (A) Schematic model for SAP. (B and C) Histological sections of H&E-stained pancreatic and lung tissue of C57BL/6 mice at the indicated time points. Note the increase of edema (asterisk) and necrosis (white arrowheads) in the pancreas after 8 hours and 3 days and the first signs of regeneration of damaged pancreatic tissue (black arrowheads) after 3 days. Lung damage continued to increase after 3 days, as demonstrated by alveolar wall thickening and collapse (see higher-magnification views of boxed regions at far right; enlarged $\times 3$). (D) MPO activity in lung tissue of C57BL/6 mice ($n = 5$). (E) Flow cytometry analysis of CD11b⁺/Gr-1⁺ cells in total lung tissue ($n = 6$) and cytospin preparation of BALF in C57BL/6 mice. (F) Lung permeability, evaluated by FITC-dextran clearance. (G) Interstitial fluid accumulation, measured as capillary-alveolar membrane thickness ($n = 10$). (H–K) Total cell count (H), total protein concentration (I), BALF CXCL1 (J), and BALF IL-6 (K) ($n = 1–3$ per condition; 4 independent experiments). (L and M) Serum levels of IL-6 (L) and CXCL1 (M) in C57BL/6 mice ($n > 5$). (N) Kaplan-Meier curves of cerulein-treated *Il6*^{-/-} mice (green; $n = 5$) and of C57BL/6 mice treated with cerulein (black; $n = 6$), cerulein plus 5 $\mu\text{g/d}$ recombinant IL-6 (blue; $n = 5$), or NaCl sham plus 5 $\mu\text{g/d}$ recombinant IL-6 (purple; $n = 5$). Results represent mean \pm SD. * $P < 0.05$, ** $P < 0.005$, *** $P < 0.001$. Scale bars: 50 μm .

Here, using genetic and pharmacological approaches in mice, we revealed the underlying mechanisms of lethal ALI during SAP and identified the IL-6 trans-signaling cascade via STAT3 as a novel molecular target for lethal ALI.

Results

A model for SAP-induced lethal ALI. The most relevant, well-established mouse model of SIRS-associated ALI is cerulein-induced AP (21, 22). Cerulein binds specifically to the acinar cell-restricted receptor CCK-A and induces pancreatic damage through intracinar activation of digestive enzymes (21). With the exception of 1 study, multiple daily injections of the CCK analog cerulein have been reported to cause nonlethal, noninfectious AP with mild ALI (23, 24). To increase multiple organ damage and lethality, we modified the cerulein model by inducing AP in mice for 5 consecutive days (Figure 1A). This protocol resulted in SAP with multiple organ damage.

Although the pancreas showed the first signs of regeneration after 3 days (Figure 1B and Supplemental Figure 1, A and B; supplemental material available online with this article; doi:10.1172/JCI64931DS1), lung damage increased dramatically over time, as shown by histological changes in the lung (Figure 1C). These changes in morphology were further emphasized by increased myeloperoxidase (MPO) activity (Figure 1D). Because MPO is detectable in neutrophils and monocytes, we performed flow cytometry experiments, which revealed that granulocytes (also known as polymorphonuclear leukocytes) were significantly increased in the lung after 8 hours of AP (Figure 1E). In addition to granulocytes, macrophages were also detected in bronchoalveolar lavage fluid (BALF) (Figure 1E and refs. 25, 26). Pulmonary damage caused by ALI is also characterized by increased alveolar permeability. Therefore, to evaluate the extent of alveolar permeability, we measured extravasation of FITC-dextran from the circulation to the alveoli, which increased significantly over time (Figure 1F). This rise might explain the observed increase in alveolar thickness (Figure 1G). In line with this observation, we found that the number of cells as well as protein content increased in BALF

(Figure 1, H and I). BALF contained increased numbers of chemokines (i.e., CXCL1; also known as KC) and cytokines (i.e., IL-6) that are known to be important for cellular recruitment and inflammation (Figure 1, J and K). To rule out hypotension and sepsis, we additionally analyzed blood pressure and endotoxin levels during SAP (Supplemental Figure 1, C–E). Moreover, we found that the effects on the liver and kidney were only transient (Supplemental Figure 1, F–J). This model of pancreatitis-associated lung injury revealed activation of the signaling pathways $\text{I}\kappa\text{B}/\text{NF-}\kappa\text{B}$, p38, and RhoA (Supplemental Figure 2, A and B), which are known to be important for mediating damage in the lung (18, 19).

Pulmonary damage was accompanied by elevated serum IL-6 and CXCL1 levels during disease onset (Figure 1, L and M). As the disease progressed, levels of IL-6 and CXCL1 returned to normal values, which suggests that these factors accumulate in the lung. Lethality in this modified SAP model approached 50% after 3 days, similar to that in humans with SAP (1).

In human SAP, serum IL-6 is a reliable marker for AP severity, but its significance in mediating ALI is unknown (12). To examine the function of IL-6 in ALI genetically, we applied this modified model to mice deficient in IL-6. Whereas *Il6*^{-/-} mice were resistant to death with SAP, 40% of wild-type C57BL/6 mice died. Conversely, single daily i.v. injections of recombinant IL-6 (5 μg ; 1 hour before the last cerulein injection) in diseased C57BL/6 mice significantly increased the death rate. Single daily injections of recombinant IL-6 (5 μg ; 1 hour before the last cerulein injection) with 8 hourly injections of NaCl (0.9%) had no effect on survival (Figure 1N). Thus, our genetic and pharmacological data clearly demonstrated that IL-6 is not just a marker, but a relevant pathophysiological mediator of lethality in SAP with lung injury.

IL-6 links pancreatitis to pulmonary damage. To determine the underlying mechanisms of IL-6 in terms of contributions to lethality during ALI, we analyzed the onset of inflammation in *Il6*^{-/-} mice. Consistent with previous reports (23), we found that genetic deletion of *Il6* increased susceptibility of the pancreas to inflammation-associated damage (Figure 2, A–C). In contrast, ALI was attenuated, as *Il6*^{-/-} mice revealed less alveolar thickness and granulocyte accumulation in the lung (Figure 2, D–F). In parallel, levels of circulating CXCL1 in *Il6*^{-/-} mice decreased significantly (Figure 2G).

The neutrophil-attracting chemokine CXCL1 has previously been shown to depend on the gp130-STAT3 axis (25). Because IL-6 also exerts its proinflammatory effects through the Jak-2-dependent STAT3 pathway, we examined whether STAT3 is activated during AP and whether its activation depends on IL-6. Using pancreatic tissue from C57BL/6 and *Il6*^{-/-} mice, we examined phosphorylation of STAT3 and STAT1 using Western blot analysis. Activation of STAT3 was clearly attenuated in *Il6*^{-/-} mice compared with wild-type controls; phosphorylation of STAT1 was not detectable in either group (Figure 2H). These findings were supported by immunohistochemistry (IHC), which demonstrated loss of p-STAT3^{Y705} in the acinar cells of *Il6*^{-/-} mice (Figure 2I, white arrowhead); conversely, the immune cells still demonstrated STAT3 activation (Figure 2I, black arrowhead). These data implicate STAT3 in the pancreas as a mediator of IL-6-dependent effects in AP-associated ALI. We therefore conclude that IL-6 links the inciting event of AP to the secondary development of ALI, potentially via STAT3 activation in the pancreas.

IL-6 trans-signaling activates STAT3 in the pancreas to mediate pulmonary damage. Next, we sought to determine the mechanisms by which IL-6 mediates STAT3 activation in the pancreas. We

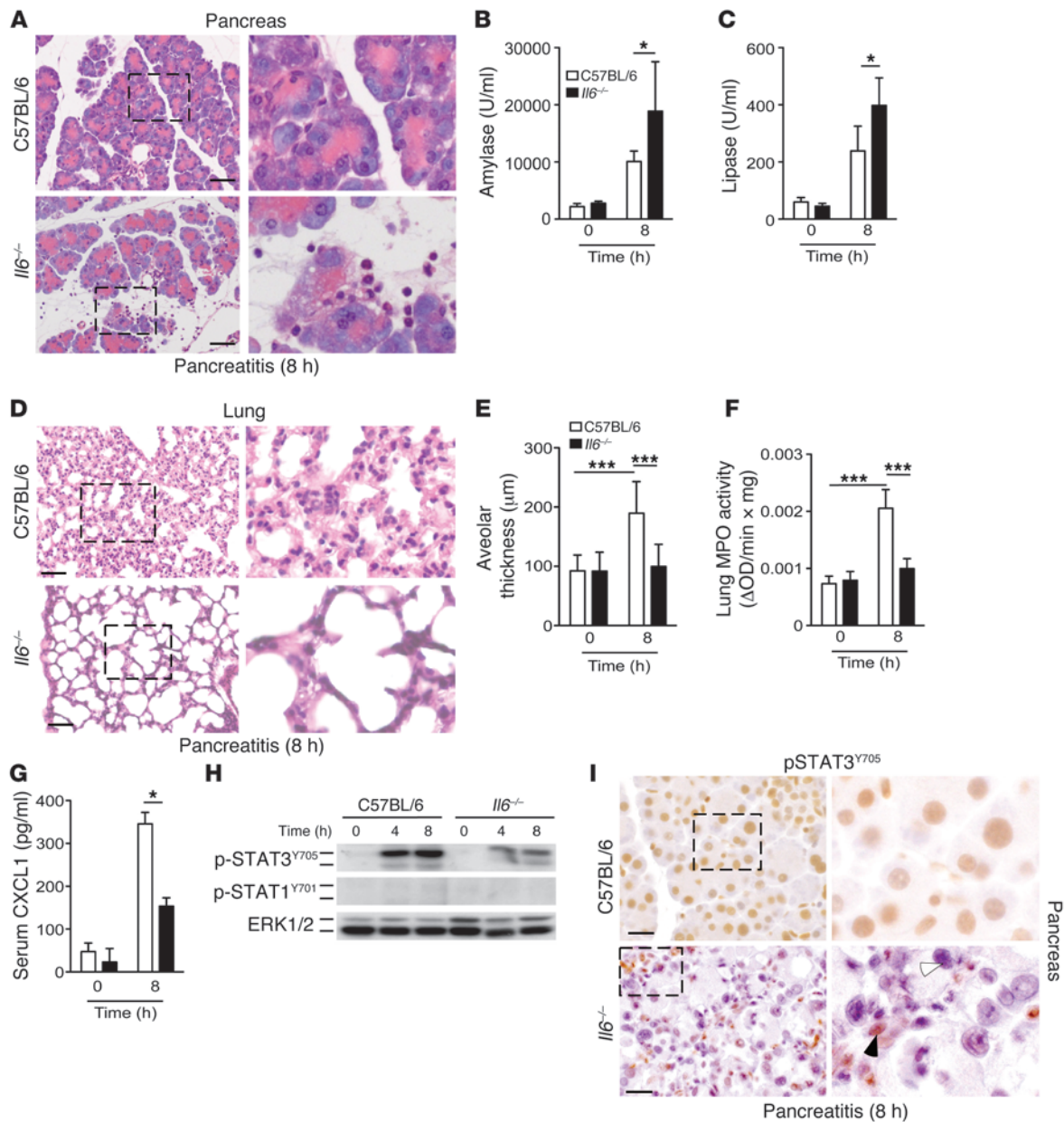


Figure 2

IL-6 is required to link pancreatic damage to pulmonary damage during AP. C57BL/6 and *Il6*^{-/-} mice were subjected to 8 hours of AP. (A) Morphological analysis of H&E-stained pancreatic tissue. (B and C) Amylase and lipase levels (*n* = 4). (D) Histological sections of lung tissue. Note the increased alveolar wall thickening and collapse in C57BL/6 mice. (E) Capillary-alveolar membrane thickness (*n* = 10). (F) MPO activity in lung tissue (*n* > 5). (G) Serum CXCL1 (*n* = 4). (H) Pancreatic tissue was isolated at the indicated time points and homogenized to detect p-STAT3^{Y705} and p-STAT1^{Y701}. ERK1/2 served as loading control (representative blot; *n* = 4 per time point). (I) IHC staining of p-STAT3^{Y705} in pancreatic tissue. Only C57BL/6 mice showed STAT3 activation in acinar cells; *Il6*^{-/-} mice showed phosphorylation of STAT3 in immune cells (black arrowhead), but not in acinar cells (white arrowhead). Results represent mean ± SD. **P* < 0.05, ****P* < 0.001. Scale bars: 50 μm. Boxed regions are shown at higher magnification at right (enlarged ×3).

therefore extended our analysis to isolated acinar cells. To test the hypothesis that IL-6 mediates STAT3 activation, we stimulated acinar cells for 2 hours with different concentrations of IL-6. Surprisingly, IL-6 alone did not induce robust STAT3 phosphorylation (Figure 3A). Notably, even supramaximal concentrations of the CCK analog cerulein failed to activate STAT3 in isolated acinar cells (Supplemental Figure 3A). IL-6 can activate STAT3 via

2 modes. The first mode entails classical signaling mechanisms characterized by binding of IL-6 to IL-6R and gp130 on specific target cells. Alternatively, IL-6 binds to the naturally occurring sIL-6R, forming a complex with IL-6 that initiates signaling in cells that lack membrane-bound IL-6R; this process is called IL-6 trans-signaling (15). To test the concept that IL-6 mediates STAT3 activation in acinar cells via IL-6 trans-signaling, we stimulated

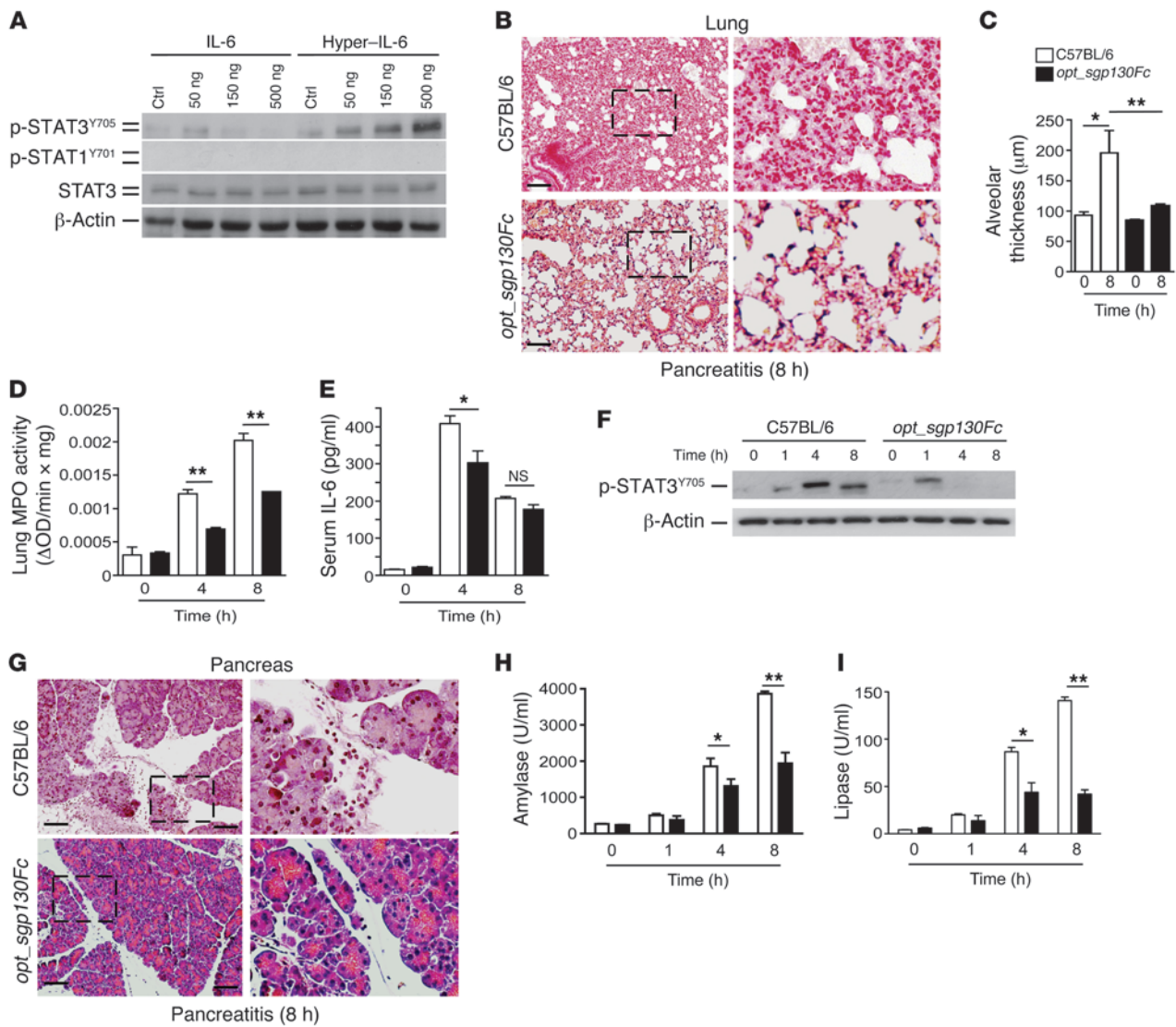


Figure 3

IL-6 trans-signaling via STAT3 mediates ALI during SAP. (A) Acinar cells were incubated with indicated concentrations of IL-6 or hyper-IL-6 for 2 hours. Protein lysates from incubated acinar cells were homogenized and blotted with p-STAT3^{Y705}, p-STAT1^{Y701}, and STAT3. β-Actin served as loading control (representative blot; n = 3). (B) Morphological analysis of representative H&E stains revealed less alveolar collapse and thickness in *opt_sgp130Fc* compared with C57BL/6 mice. (C) Interstitial fluid accumulation, measured as capillary-alveolar membrane thickness (n = 5). (D) Lung tissue was removed to measure MPO activity (n = 5). (E) Serum IL-6 concentration (n = 4). (F) Pancreatic tissue was isolated at the indicated times and homogenized to detect p-STAT3^{Y705}. β-Actin served as loading control (representative blot; n = 4 per time point). (G) Morphological analysis of representative H&E stains revealed less pancreatic injury in *opt_sgp130Fc* compared with C57BL/6 mice. (H and I) Serum analysis showed significantly lower levels of amylase and lipase after 4 and 8 hours in *opt_sgp130Fc* versus C57BL/6 mice. Results represent mean ± SD. *P < 0.05, **P < 0.005. Scale bars: 50 µm. Boxed regions are shown at higher magnification at right (enlarged ×3).

acinar cells for 2 hours with different concentrations of the fusion protein hyper-IL-6, which consists of IL-6 and sIL-6R (27). Indeed, only hyper-IL-6 was sufficient to induce STAT3 phosphorylation in isolated acinar cells in vitro (Figure 3A). Conversely, hepatocytes expressing membrane-bound IL-6R responded to IL-6 (data not shown and ref. 28). In fact, unlike hepatocytes, acinar cells showed only weak expression of membrane-bound IL-6R (data not shown). In contrast, circulating levels of sIL-6R in serum increased during pancreatitis onset and returned to normal as the disease progressed (Supplemental Figure 3B). However, sIL-6R in BALF

continued to increase during the course of disease (Supplemental Figure 3C). Such kinetics and distribution resembled those of IL-6 and CXCL1. Taken together, our in vitro data indicate that IL-6 trans-signaling, rather than classical IL-6 signaling, is required to activate STAT3 in acinar cells.

Prior research has shown that IL-6 trans-signaling plays a significant role in regulating leukocyte recruitment, a process required for ALI (29, 30). Thus, we next sought to determine whether specific inhibition of IL-6 trans-signaling in vivo has effects on ALI similar to those of *Il6*^{-/-} mice. We used *opt_sgp130Fc* mice, a line

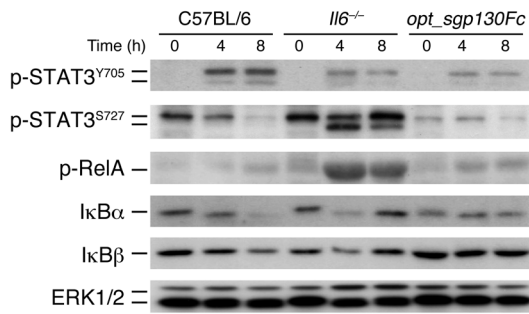


Figure 4
Classical IL-6 signaling and IL-6 trans-signaling activate different pathways in the pancreas during inflammation. At 0, 4, and 8 hours, pancreatic tissue from C57BL/6, *Il6*^{-/-}, and *opt_sgp130Fc* mice was isolated and homogenized to detect p-STAT3^{Y705}, p-STAT3^{S727}, p-RelA, IκBα, and IκBβ. ERK1/2 served as loading control (representative blot; *n* = 4 per time point).

with liver-specific transgenic overexpression of a soluble gp130Fc (*sgp130Fc*); more specifically, *sgp130Fc* inhibits IL-6 trans-signaling without affecting classical IL-6 signaling (17, 31).

Overexpression of *sgp130* alleviated the extent of ALI during AP (Figure 3, B–D); circulating levels of IL-6 were still high, but with a significant difference after 4 hours (Figure 3E). This was accompanied by attenuated STAT3 activation in *opt_sgp130Fc* mice (Figure 3F). In contrast to findings in *Il6*^{-/-} mice, local pancreatic inflammation was attenuated (Figure 3, G–I), which suggests that IL-6 trans-signaling, rather than classical IL-6 signaling, is involved in the mediation of pancreatic damage. Collectively, these data demonstrated that IL-6 trans-signaling, not classical IL-6 signaling, links the inciting event of AP to the secondary development of ALI. Our data also implicated IL-6 trans-signaling-dependent STAT3 activation as the linking module.

Classical IL-6 signaling and IL-6 trans-signaling activate distinct pathways in the pancreas during inflammation. Although pulmonary damage was attenuated in *Il6*^{-/-} and *opt_sgp130Fc* mice, the extent of local damage in the pancreas differed. To better understand the mechanisms underlying these findings, we analyzed various signaling pathways involved in AP in vivo. Interestingly, whereas STAT3^{Y705} phosphorylation was clearly diminished in *Il6*^{-/-} and *opt_sgp130Fc* mice, serine phosphorylation at S727, which is known to attenuate ROS release from the electron transport chain (32), was dramatically increased in *Il6*^{-/-} mice (Figure 4), suggestive of increased ROS. This was not true for C57BL/6 and *opt_sgp130Fc* mice. Furthermore, *Il6*^{-/-} mice revealed strong phosphorylation of RelA in the pancreas. Likewise, the inhibitor proteins IκBα and IκBβ rapidly degraded. Transgenic *opt_sgp130Fc* mice revealed only slight activation of the IκB/NF-κB cascade. IκBα and IκBβ degradation was most prominent after 8 hours. In summary, although inhibition of classical IL-6 signaling and IL-6 trans-signaling both reduced p-STAT3^{Y705} in vivo, they implicated different pathways in the pancreas during inflammation. These findings might explain the different phenotypes in the pancreases of *Il6*^{-/-} and *opt_sgp130Fc* mice.

Myeloid cells secrete IL-6 in a NF-κB-dependent manner. To further specify the cellular source of increased NF-κB activation, we performed IHC staining. NF-κB activation at this time point was mostly restricted to infiltrating cells (Figure 5, A and B). In addition to NF-κB, myeloid cells were ultimately revealed as the cel-

lular source of local and systemic IL-6 (Figure 5C). While NF-κB in acinar cells has been shown to be involved in inflammation in numerous studies, its role in myeloid cells has not been addressed in this context (21, 33). To investigate the role of myeloid RelA/p65 in IL-6 regulation, we generated a mouse line that lacked functional active RelA/p65 in macrophages and granulocytes (referred to herein as *RelA*^{Δmye} mice; Figure 5D). LysM-Cre-driven inactivation of RelA/p65 prevented much of the late increase in NF-κB activity (Figure 5E), further corroborating the evidence that myeloid cells are the major source of IL-6 at this time point. Early activity of NF-κB was not significantly different in either mouse line (data not shown). Interestingly, the release of pancreatic amylase did not change (data not shown), even though ALI in *RelA*^{Δmye} mice was greatly reduced (Figure 5F). *RelA*^{Δmye} mice displayed less circulating IL-6; moreover, mRNA levels of *Il6* and *Cxcl1* were also reduced in the pancreas (Figure 5, G–I). In addition, pancreatic phosphorylation of STAT3^{Y705} after cerulein exposure in *RelA*^{Δmye} mice was attenuated (Figure 5J). Collectively, these data indicated that RelA/p65-dependent IL-6 secretion in myeloid cells contributes to phosphorylation of STAT3^{Y705}. Furthermore, inactivation of RelA/p65 in myeloid cells uncouples local damage from ALI during AP.

Phosphorylation of STAT3^{Y705} modulates inflammation severity and determines lethality. To define the requirements for STAT3/SOCS3 in the pancreas to mediate lethal ALI, we generated mice in which STAT3 or SOCS3 was deleted in the pancreas (referred to herein as *Stat3*^{Δpanc} and *Socs3*^{Δpanc} mice, respectively; ref. 34). This Cre/loxP-based system affected recombination in the pancreas, but not the liver or lung (Figure 6A and Supplemental Figure 4, A and B). Expression of p-STAT^{Y705} was completely abrogated in *Stat3*^{Δpanc} mice, whereas *Socs3*^{Δpanc} mice revealed strong and sustained phosphorylation of STAT3^{Y705} (Figure 6, B and C). Local damage was attenuated in *Stat3*^{Δpanc} mice, but was aggravated in *Socs3*^{Δpanc} mice, as shown by histology, amylase and lipase levels, relative pancreatic weight, and CXCL1 levels (Figure 6, D–F, and Supplemental Figure 4, C and D). Because intra-acinar conversion of trypsinogen to trypsin is believed to influence acinar cell death, we next measured trypsin activity in all mouse lines during AP. Early trypsin activity was not different in any mouse line. Surprisingly, late trypsin activity was even inversely correlated to p-STAT3^{Y705} (Figure 6G). AP severity in *Stat3*^{Δpanc} and *Socs3*^{Δpanc} mice was accompanied by decreased and increased serum IL-6 levels, respectively (Figure 6H).

Histopathological examination of *Stat3*^{Δpanc} lungs after serial injections of cerulein demonstrated limited inflammatory cell influx and preservation of the alveolar structure; in contrast, these features were pronounced in *Socs3*^{Δpanc} mice (Figure 7A). In accordance with this observation, all indices – including MPO activity, lung edema, tissue permeability, and alveolar thickness – were dependent on phosphorylation of STAT3^{Y705} in the pancreas, as they were substantially reduced in *Stat3*^{Δpanc} mice and increased in *Socs3*^{Δpanc} mice (Figure 7, B–E). Analysis of BALF revealed reduced pulmonary damage in *Stat3*^{Δpanc} mice as the disease progressed. Total protein, IL-6, and CXCL1 levels in BALF were attenuated in *Stat3*^{Δpanc} mice (Figure 7, F–H). *Socs3*^{Δpanc} mice were not available at this time point because all of them succumbed to SAP; in contrast, STAT3-knockout mice were resistant to SAP-induced lethal ALI (Figure 7I). Together, these observations support the assertion that phosphorylation of STAT3^{Y705} determines the severity of local and pulmonary inflammation during AP.

Pharmacological inhibition of STAT3 and IL-6 trans-signaling mitigate SAP-induced lethal ALI. These observations raised the possibility

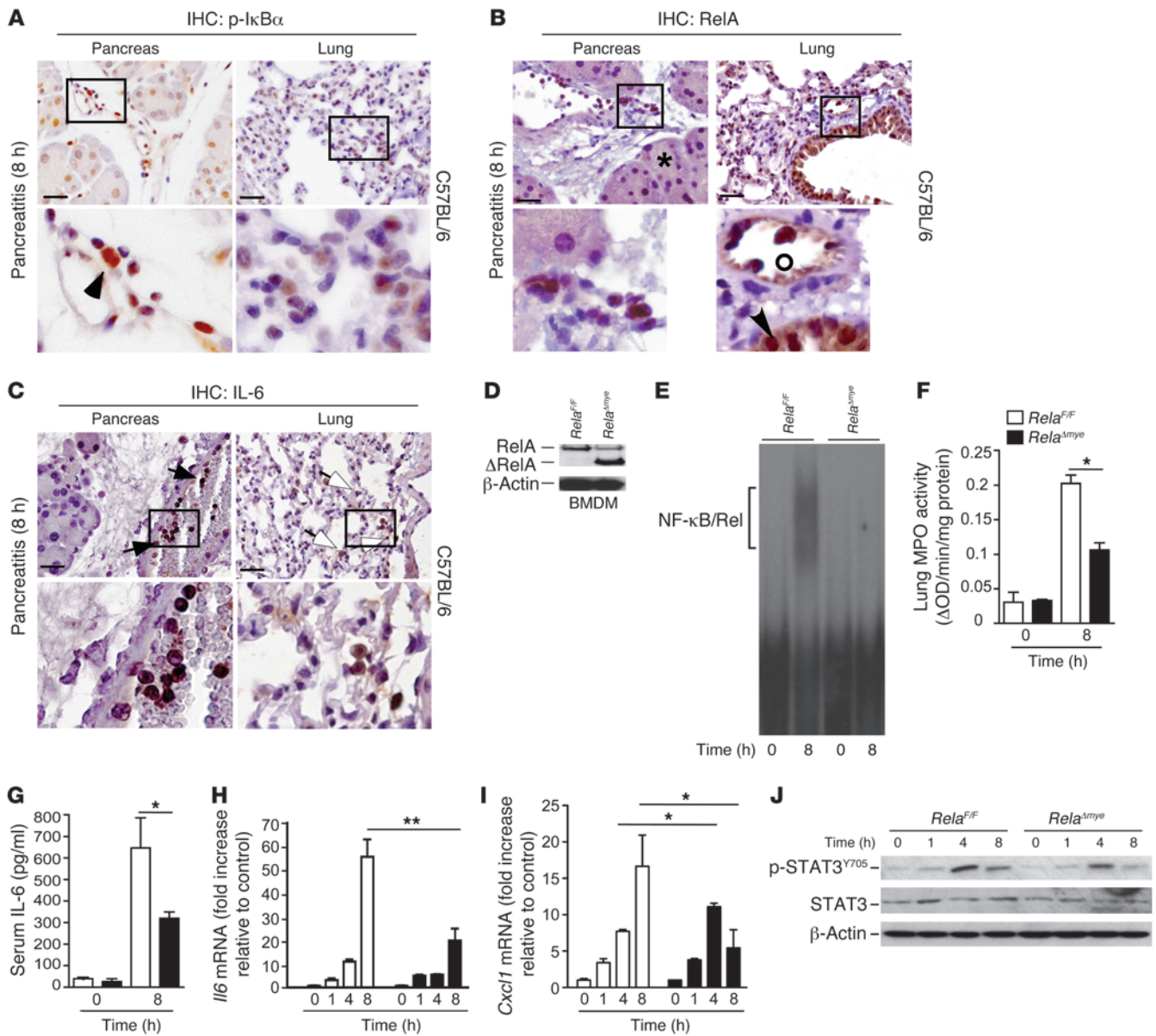


Figure 5

Myeloid cells secrete IL-6 in a NF-κB-dependent manner. (A and B) Immunohistochemical analyses were used to localize p-IκBα (A) and RelA/p65 (B) in pancreas and lung tissues 8 hours after the first injection of cerulein. Positive results for p-IκBα and RelA/p65 in the pancreas (black arrowheads) were mainly restricted to inflammatory cells. Acinar cells remained negative (asterisk). (A) Alveolar cells showed weak activation of p-IκBα. (B) Bronchial epithelium (arrowhead) and infiltrating cells (circle) in the lung harbored nuclear RelA/p65. (C) IHC analyses were used to localize IL-6 in the pancreas and lung. Positive results for IL-6 in the pancreas were strictly restricted to inflammatory cells (black arrows). Alveolar macrophages expressed IL-6 in the lung (white arrows). (D) Myeloid-specific abrogation of RelA/p65 in bone marrow-derived macrophages (BMDM) of *Rela^{F/F}* and *Rela^{Δmye}* mice. (E) Pancreatic nuclear protein extracts (10 μg) were subjected to gel retardation assays with an NF-κB consensus binding site (representative EMSA; n = 4). (F) Lung tissue was removed to measure MPO activity (n = 4). (G–I) Serum was removed for IL-6 evaluation (G), and levels of *Il6* (H) and *Cxcl1* (I) mRNA of total pancreatic mRNA were determined, in *Rela^{F/F}* and *Rela^{Δmye}* mice. Fold change values (± SD) were normalized to *cyclophilin* mRNA (n = 4). (J) Pancreases were harvested and homogenized to detect p-STAT3^{Y705}. STAT3 and β-actin served as loading controls (representative blot; n = 4). Results represent mean ± SD. *P < 0.05, **P < 0.005. Scale bars: 50 μm. Boxed regions are shown at higher magnification below (enlarged ×3).

that pharmacological inhibition of IL-6 trans-signaling and its downstream effector, STAT3, as well as of CXCL1 and its receptor, CXCR2, can prevent SAP-linked lethal ALI. To examine this hypothesis, C57BL/6 mice were subjected to the SAP model and injected with recombinant sgp130Fc, the small-molecule STAT3

inhibitor S3I-201, the CXCR2 antagonist SB225002, or the anti-CXCL1 antibody (Supplemental Figure 5A). S3I-201 specifically inhibited nuclear translocation of phosphorylated STAT3 in vivo (Supplemental Figure 5B and ref. 35). Administration of sgp130Fc, SB225002, anti-CXCL1 antibody, and S3I-201 saved

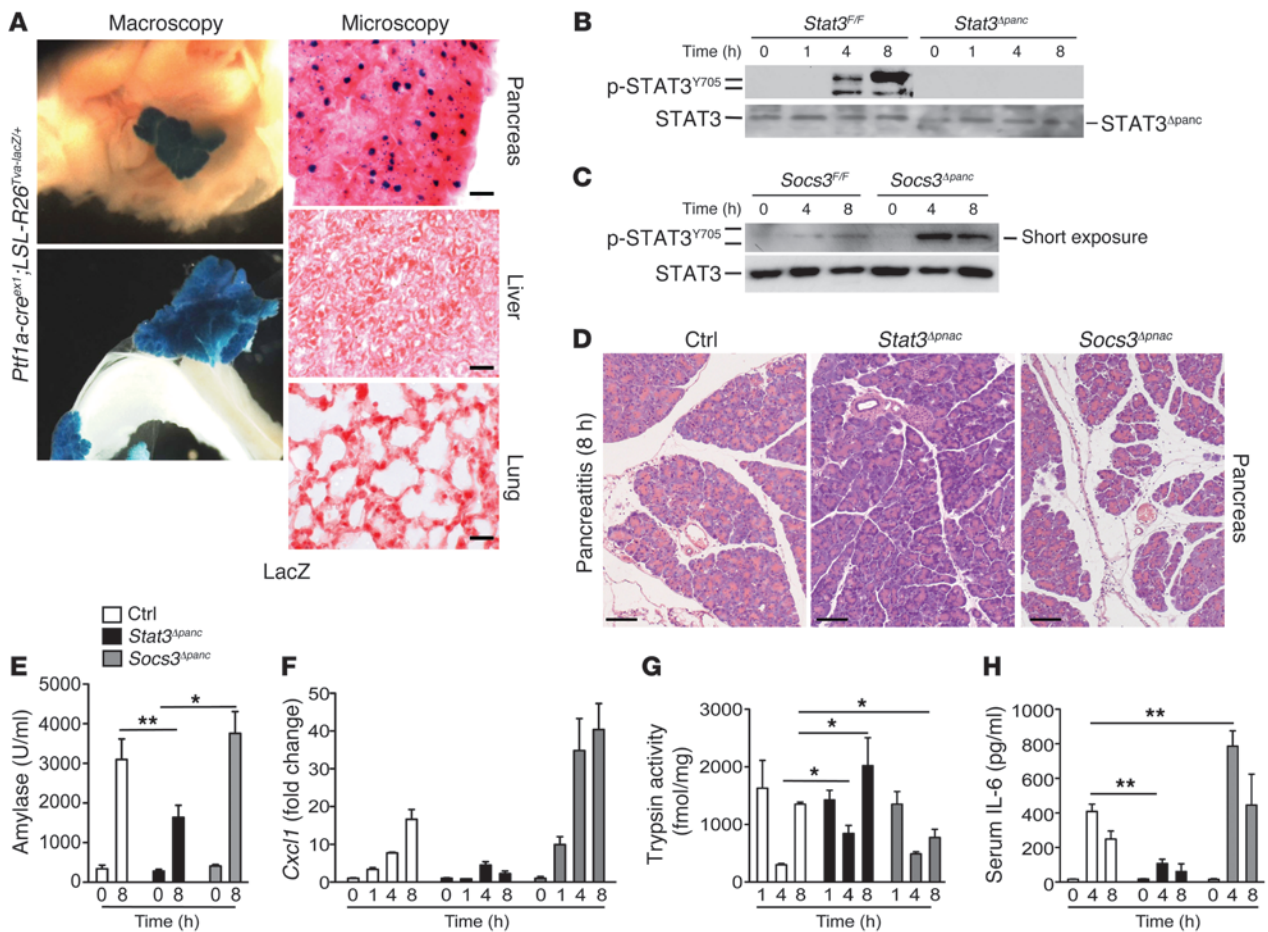


Figure 6 Pancreas-specific p-STAT3^{Y705} modulates the severity of local inflammation during AP. (A) Macroscopic images of X-gal–stained liver, pancreas, and small bowel. Microscopic images of nuclear lacZ activity in sections of pancreas, liver, and lung. (B) Pancreases were isolated to detect p-STAT3^{Y705} during AP. Note the absence of STAT3 activation in *Stat3^{Apanc}* mice. STAT3 served as loading control (representative blot; *n* = 5). Truncated STAT3 protein in the pancreas (STAT3^{Apanc}) is indicated. (C) Pancreases were subjected to Western blot analysis using a p-STAT3^{Y705}–specific antibody. Note the increased p-STAT3^{Y705} in *Socs3^{Apanc}* mice. STAT3 served as a loading control (representative blot; *n* = 5 per time point). (D) Morphological analysis of pancreases after 8 hours of AP in the indicated mice. (E) Serum was removed for amylase measurement at the indicated time points. Note the increased release of amylase into the serum in *Socs3^{Apanc}* mice, while levels remained lower in *Stat3^{Apanc}* mice compared with controls (*Stat3^{F/F}* and *Socs3^{F/F}*). (F) Levels of *Cxcl1* mRNA of total pancreatic mRNA in control, *Stat3^{Apanc}*, and *Socs3^{Apanc}* mice. Fold change values (± SD) were normalized to *cyclophilin* mRNA (*n* > 3). (G) Early trypsin activation was independent of STAT3 activation (*n* = 8). (H) Serum IL-6 levels at the indicated time points. Values are mean ± SD for independent animals (*n* = 5). **P* < 0.05, ***P* < 0.005. Scale bars: 100 μm.

all animals from SAP-induced ALI (Figure 8A). Even CXCL1 and CXCR2 were relevant for pancreatitis-associated lung injury: blocking of CXCR2 by use of SB225002 or an antibody directed against CXCL1 protected mice completely from death. Notably, although we observed no changes in local damage (Figure 8, B, C, and E), pulmonary injury significantly improved in all treatment groups (Figure 8, D and F). These data demonstrated the importance of the IL-6/STAT3/CXCL1 pathway in linking the inciting event of AP to acute pulmonary damage.

Our findings indicated that the IL-6 trans-signaling–dependent STAT3 pathway is central to AP-associated lethal ALI and may thereby represent a potential therapeutic target. Therefore, we next evaluated the clinical relevance of these data (Supplemental Table 1) using plasma from individuals with AP. Because levels of IL-6 decrease as AP progresses, plasma was drawn within 50 hours of disease onset for both groups of patients (Figure 9A and refs. 12,

36). Similar to previous reports, IL-6 levels were significantly higher in plasma from individuals with ALI compared with patients with mild AP and control subjects (Figure 9B and ref. 12). However, the association between IL-6/sIL-6R and ALI was significant (Figure 9, C and D, and ref. 37), reliably distinguishing patients with mild AP from those with pancreatitis-associated organ/lung failure. IL-8, a human ELR⁺ CXC chemokine that activates neutrophils (e.g., mouse CXCL1), was significantly elevated in plasma of patients with SAP and organ failure (Figure 9E and refs. 38, 39). These findings highlighted the activity of the IL-6 trans-signaling/STAT3/CXCL1 cascade in patients with pancreatitis-associated organ failure.

Discussion

The causal link between the inflammatory process of SAP and concomitant evolving lethal ALI has long been recognized in daily clinical practice; however, the underlying molecular mechanisms

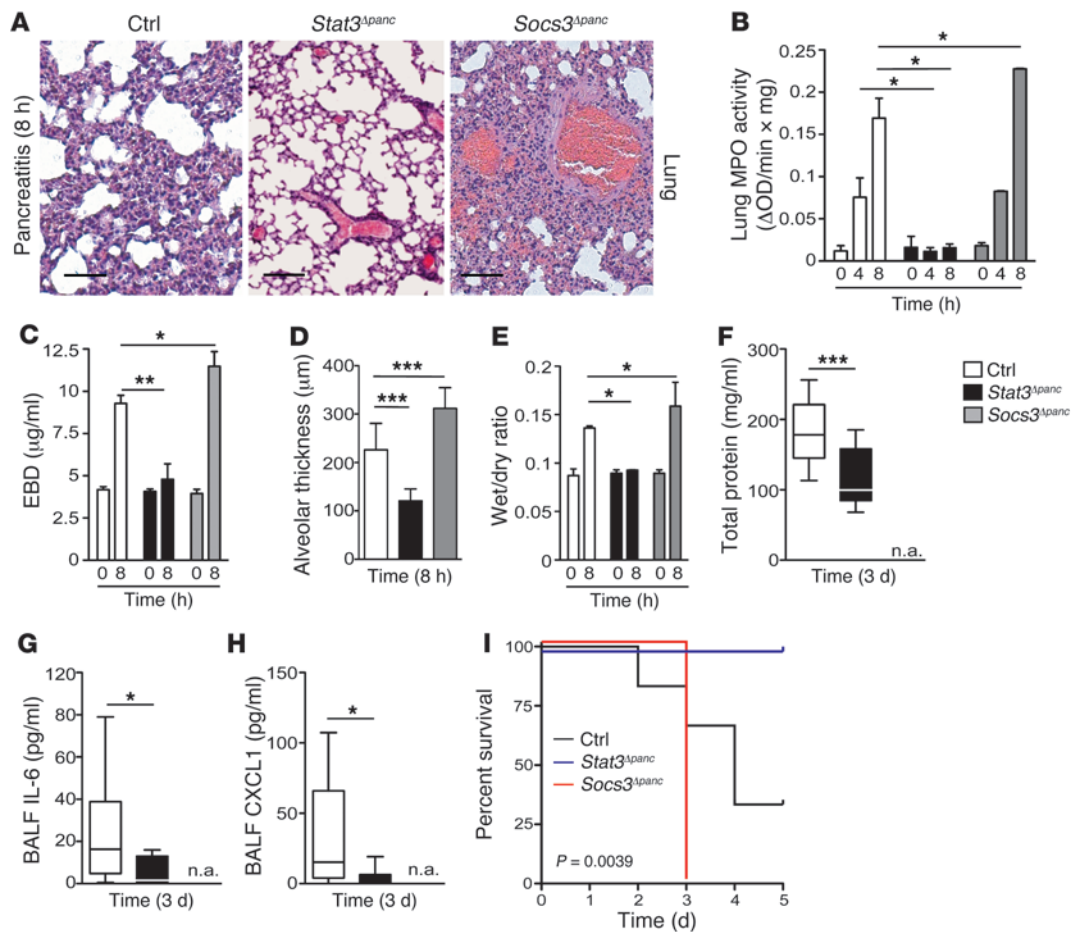


Figure 7

Phosphorylation of STAT3 in the pancreas contributes to systemic complications. (A) Histological sections of lung tissue from control, *Stat3^{Δpanc}*, and *Socs3^{Δpanc}* mice revealed marked hemorrhage and alveolar collapse in *Socs3^{Δpanc}* mice. (B) MPO activity in lung tissue of control, *Stat3^{Δpanc}*, and *Socs3^{Δpanc}* mice at the indicated time points during AP (*n* = 6). (C) Lung permeability, determined by injection of EBD in the right femoral artery and measurement of dye concentration in lung tissue at 0 and 8 hours (*n* = 4). (D) Interstitial fluid accumulation, determined by capillary-alveolar membrane thickness. Values represent mean ± SD (*n* = 10). (E) Lung edema, determined indirectly by the increase in pulmonary fluid accumulation (*n* = 8). Animals were killed at 8 hours, and the left lung was removed in order to determine the wet/dry ratio (*n* = 8). (F–H) Protein concentration (F), IL-6 (G), and CXCL1 (H) measured in BALF taken from control and experimental animals (*n* = 4; 1–3 BALF/animal). Note that BALF could not be taken from *Socs3^{Δpanc}* mice (n.a.), since all mice died due to SAP. (I) p-STAT3^{Y705} was linked to SAP-induced lethal ALI. Kaplan-Meier curves of control (*n* = 6), *Stat3^{Δpanc}* (*n* = 9), and *Socs3^{Δpanc}* (*n* = 5) mice during SAP. Values represent mean ± SD. **P* < 0.05, ***P* < 0.005, ****P* < 0.001. Scale bars: 50 μm.

remained unclear. Using tissue-specific gain- and loss-of-function approaches in a mouse model of SAP and ALI, we here provided direct genetic and pharmacological evidence that IL-6 trans-signaling, not classical IL-6 signaling, linked the inciting event of SAP to the secondary development of ALI. In terms of the underlying mechanisms, we found that IL-6 formed complexes with sIL-6R to activate STAT3 in the pancreas, thus amplifying inflammation by further releasing proinflammatory factors during SAP. IL-6 secretion at the site of inflammation was controlled by NF-κB in the nuclei of recruited myeloid cells. Persistent STAT3 activation resulted in high levels of CXCL1 that mediated granulocyte infiltration into the lung, promoting lethal ALI. This axis appeared to be present in individuals with SAP and ALI, which suggests that the mechanism exists across species.

While the role of IL-6 in AP has been extensively analyzed, IL-6-trans-signaling has not been addressed in this context (23, 40).

We previously showed that inactivation of NF-κB in the pancreas increased local damage and aggravated ALI, which was accompanied by high systemic and local levels of IL-6 (21, 33). Here, we demonstrated the role of IL-6 trans-signaling in SAP and ALI, showing that IL-6 is not merely a marker, but a relevant pathophysiological player in the disease process (12, 13). Our results showed that IL-6 exerted its effects during SAP and lethal ALI predominantly via IL-6 trans-signaling. This type of activation rendered virtually all cells capable of responding to IL-6/sIL-6R complexes. Moreover, we demonstrated IL-6 trans-signaling to regulate processes localized to the site of inflammation. This mode of activation enhanced IL-6 responsiveness and drove inflammatory events. In addition to its proinflammatory capacities, classical IL-6 signaling coordinated homeostatic properties of IL-6, such as neutropenia, changes in cholesterol, and weight gain (31). Beyond phosphorylation of STAT3^{Y705}, classical IL-6 signaling and

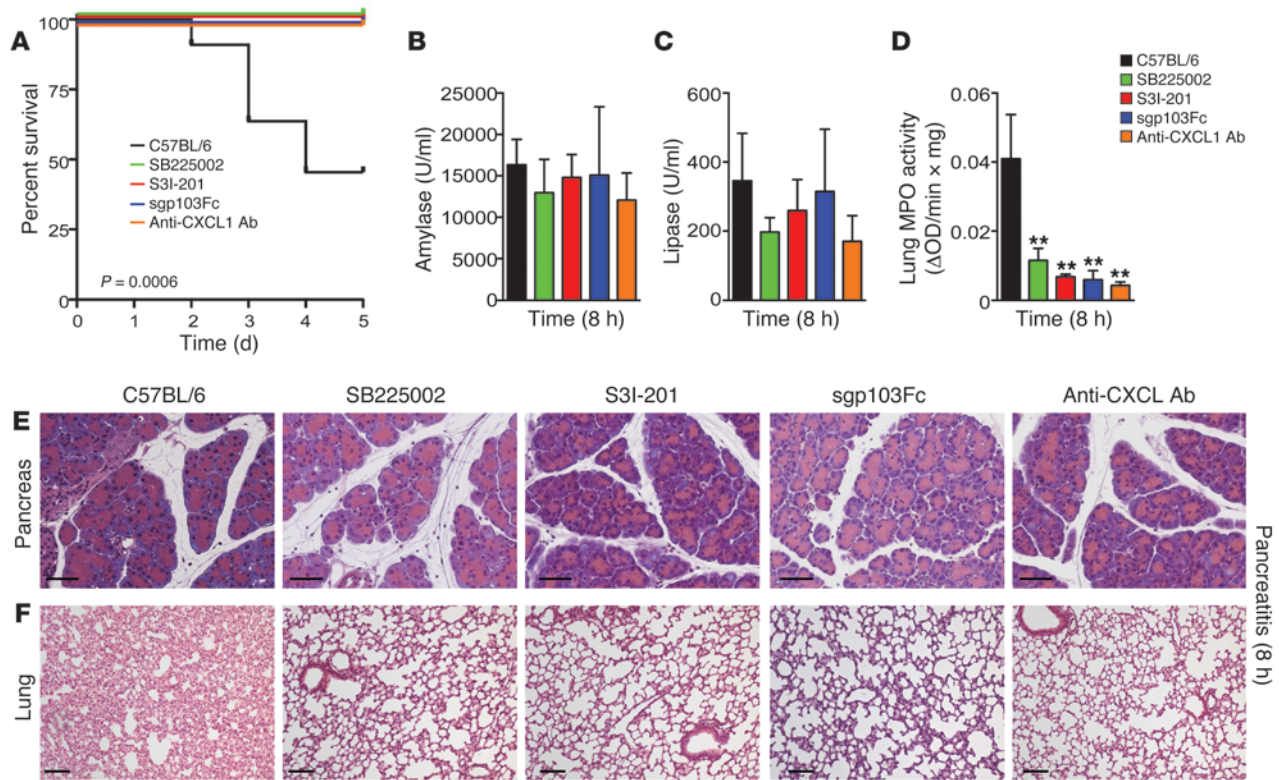


Figure 8 Pharmacological inhibition of STAT3, CXCR2, CXCL1, and IL-6 trans-signaling attenuates SAP-induced lethal ALI. (A) Kaplan-Meier curves of C57BL/6 mice (black; $n = 11$) and C57BL/6 mice treated with the CXCR2 antagonist SB225002 (green; $n = 12$), the STAT3 inhibitor S3I-201 (red; $n = 7$), recombinant sgp130Fc (blue; $n = 8$), or an anti-CXCL1 antibody (orange; $n = 5$) during SAP. (B and C) Serum was removed for amylase and lipase analyses at the indicated time points ($n = 4$). (D) MPO activity in lung tissue of C57BL/6 mice or treated mice 8 hours after the first cerulein injection ($n = 4$). (E and F) Histological sections of pancreatic and lung tissue. Note the decrease in lung injury in treated versus C57BL/6 mice. ** $P < 0.005$ versus control. Scale bars: 50 μm (E); 100 μm (F).

IL-6 trans-signaling are likely involved in distinct and different pathways during inflammation (41). More importantly, IL-6 was found to play a crucial antiinflammatory role in both local and systemic acute inflammatory responses by controlling the level of proinflammatory, but not antiinflammatory, cytokines. In fact, we observed strong phosphorylation of STAT3^{S727} and of RelA in the pancreatic tissue of *Il6*^{-/-} mice; this phosphorylation was not detectable in control or transgenic *opt_sgp130Fc* mice. Phosphorylation of STAT3^{S727}, for example, was found to be localized in the mitochondria, for optimal function of the electron transport chain (32). Whether this phosphorylation accounts for the severe local damage in *Il6*^{-/-} mice remains unclear. These data suggest that, unlike blocking IL-6 trans-signaling, genetic inhibition of classical IL-6 signaling likely eliminates protective mechanisms during inflammation. These observations might account for the different phenotypes observed in *Il6*^{-/-} and *opt_sgp130Fc* mice.

In addition, *Il6*^{-/-} mice revealed strong activation of the NF- κ B pathway. IHC showed that in addition to acinar cells, myeloid cells displayed strong NF- κ B activation. Using genetic tools, we further showed that myeloid NF- κ B activation contributed significantly to IL-6 synthesis and IL-6 trans-signaling, and functional inactivation of RelA/p65 in myeloid cells attenuated STAT3 phosphorylation and decreased transcriptional levels of CXCL1 and IL-6. Our data clarified previous observations and demonstrated that, unlike RelA

in acinar cells, NF- κ B/RelA in myeloid cells linked local inflammation to ALI in AP via IL-6/sIL-6R, thereby placing IL-6 trans-signaling in a central position for inflammation-associated ALI (21, 33).

By virtue of phosphorylating STAT3^{Y705}, IL-6/sIL-6R regulates leukocyte recruitment, thereby contributing to local inflammation. In response to IL-6/sIL-6R, STAT3 is activated in endothelial cells to produce chemokines and upregulate adhesion molecules (30, 42). In the pancreas, we found a number of increased proinflammatory cytokines and chemokines, some of which have been validated by other studies as STAT3 target genes; moreover, high expression of proinflammatory cytokines and chemokines was found to correlate with AP severity in animal models as well as in humans. Indeed, the neutrophil chemoattractant chemokine CXCL1, which is involved in monocyte/granulocyte traffic across endo- and epithelial barriers (26, 43, 44), was highly upregulated during SAP. Our genetic data suggest that IL-6 trans-signaling-induced STAT3 phosphorylation in the pancreas acts as an amplifier for CXCL1 induction. The ELR⁺ CXC chemokine CXCL1 binds to the CXCR2 receptor to orchestrate extravasation of leukocytes from the vascular system to the site of inflammation. In our murine model of pancreatitis-associated ALI, inhibition of CXCL1 or of the CXCR2 receptor was sufficient to prevent death independent of local damage in the pancreas. Herein, we demonstrated the pivotal role of the STAT3-dependent CXCL1/CXCR2 axis in link-

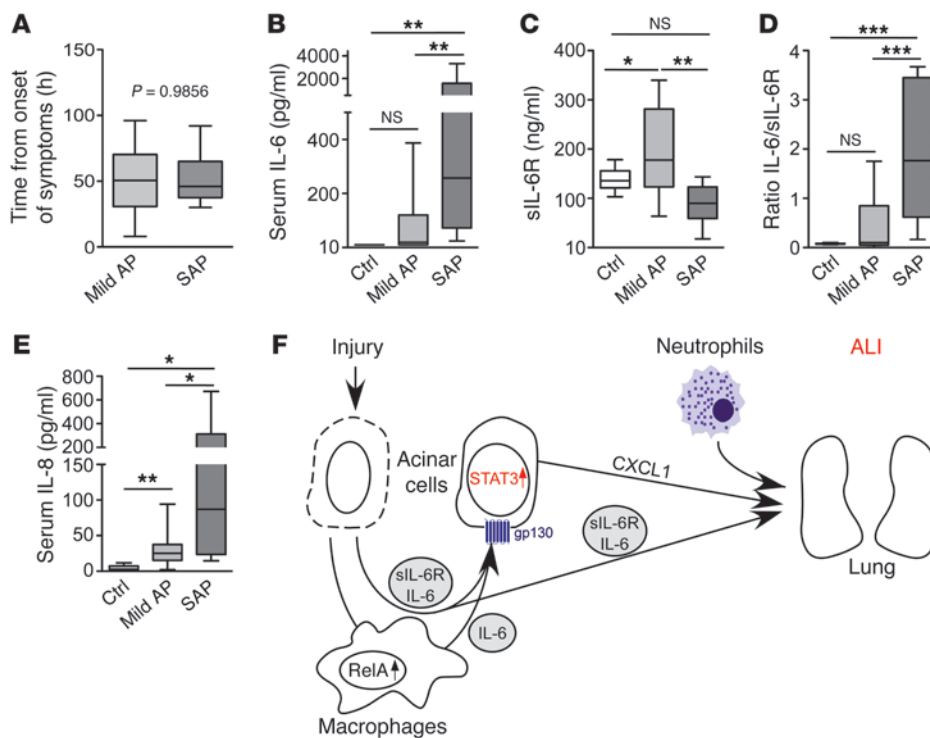


Figure 9 IL-6 trans-signaling in patients with AP. (A) Sampling of blood in individuals with mild AP and SAP after the onset of symptoms. (B and C) Serum IL-6 and sIL-6R levels in control patients and patients with mild AP and SAP. (D) IL-6/sIL-6R ratio. (E) Serum IL-8 levels in control patients and patients with mild AP and SAP. (F) Central role of IL-6 trans-signaling during SAP-associated ALI. Results represent mean \pm SD ($n > 6$). * $P < 0.05$, ** $P < 0.005$, *** $P < 0.001$.

ing pancreatic damage to ALI. Interestingly, this concept seems to be relevant even in other settings of ALI (45).

Although we observed high levels of IL-6 in patients with SAP and concomitant ALI, levels of sIL-6R were significantly lower compared with individuals with noncomplicative AP or control subjects. This potentially reflects complexation of IL-6 with sIL-6R, providing evidence in support of IL-6 trans-signaling even in the human disease. We further demonstrated that the serum IL-6/sIL-6R ratio was useful to distinguish patients with mild pancreatitis from those with SAP and subsequent ALI. Similar to IL-6, levels of the human ELR⁺ CXC chemokine IL-8 were found to be significantly higher in patients with SAP. Although human data were preliminary and need to be confirmed in larger studies with consistent time points, these data corroborated the assertion that the IL-6/STAT3/CXCL1 (IL-8) cascade is important in promoting ALI during AP. Interestingly, analysis of BALF from patients with ALI also showed elevated levels of sIL-6R, IL-6, and IL-8 (46), which suggests that this cascade exerts its effect in the lung. Whether the circulating IL-6/sIL-6R complex is sufficient to create all these effects or whether it requires additional local release of IL-6 and sIL-6R from activated neutrophils remains to be determined (29).

Our present data increase the understanding of distantly mediated ALI and help to define the function of IL-6 trans-signaling in this disease. While various approaches to inhibiting IL-6 trans-signaling and its downstream effectors during lethal AP support this model, we cannot exclude the secondary effects of intestinal permeability or increased blood pressure. Regardless, this cascade is a specific and promising target that links local inflammation to respiratory failure, meriting additional studies to examine this mechanism in other SIRS-associated diseases (47). In the present study, we demonstrated the significance of the IL-6 trans-signaling/STAT3/CXCL1 pathway in pancreatitis-associated ALI across species and how distant organ damage was linked to lethal ALI

(Figure 9F and ref. 48). This cascade not only defines a specific and promising target linking local events to systemic inflammation, its activation opens a therapeutic window, especially in patients with ongoing SAP and ALI. Yet, as previously stated, whether the circulating IL-6/sIL-6R complex is sufficient to promote these effects or whether it requires additional local release of IL-6 and sIL-6R from activated neutrophils remains to be determined (29). With the development of STAT3 inhibitors, specific IL-6/IL-6R antibodies, and soluble recombinant gp130 proteins at hand, we can reasonably test such substances in patients with SAP and ALI (35, 49).

Methods

Animal models. To delete *Stat3* or *Socs3* in the pancreas, we crossed *Stat3^{F/F}* and *Socs3^{F/F}* to *Ptf1a-cre^{ex1}* knockin mice, which were intercrossed to generate compound mutant *Ptf1a-cre^{ex1};Stat3^{F/F}* (*Stat3^{Δpanc}*) and *Ptf1a-cre^{ex1};Socs3^{F/F}* (*Socs3^{Δpanc}*) mice, respectively. Pancreas-specific expression of Cre recombinase was visualized by crossing *Ptf1a-cre^{ex1}* knockin mice to the *LSL-R26^{Tva-lacZ/+}* reporter mouse strain. *opt_sgp130Fc* transgenic mice have been previously described (17, 34). For myeloid-specific deletion of exons 7–10 in the *Rela* gene, *Rela^{F/F}* mice were crossed to the LysMCre transgenic mouse line to obtain myeloid-specific inactivation of RelA/p65 (*Rela^{Δmye}* mice) (50). In all experiments, experimental mice were compared with littermate controls of the same genetic background. C57BL/6 mice were obtained from Charles River.

Assessment of pulmonary capillary permeability. Lung permeability was determined by injection of Evans blue dye (EBD; 20 ml/kg) in the right femoral artery 30 minutes before termination of the experiment to assess vascular leakage in the lung. After mice were sacrificed, the lung was flushed with saline (0.9%), removed, and placed in formamide (2–3 ml/100 mg lung). Lungs were removed, weighed, and pooled in a tube of formamide (2–3 ml/100 mg lung). The tube was incubated at 50°C for 72 hours. EBD was extracted, and relative EBD concentration in the supernatant (compared with the standard curve) was measured at 632 nm.



To measure airway permeability, mice were challenged with cerulein for 8 hours. Along with the last i.p. injection of cerulein, mice were injected i.v. with 200 µl (5 mg/ml) of fluorescein isothiocyanate-dextran (FD4; Sigma-Aldrich). Mice were sacrificed, BALF was recovered, and alveolar permeability was measured via fluorescence.

BALF analysis. Protein content, total cell count, and inflammatory markers CXCL1 and IL-6 were analyzed in BALF. Briefly, animals were killed by decerebration. The trachea was then exposed and intubated with a catheter, and between 1 and 3 repeated injections of PBS (0.8 ml) were given to harvest BALF. Collected BALF was centrifuged at 300 g for 10 minutes at 4°C, and the supernatant was frozen at -80°C for subsequent analysis of total protein count (Bio-Rad protein analysis kit) and inflammatory mediators. Cells in the pellet were resuspended in PBS for quantification.

Models of AP. The model of experimental AP was performed as previously described (21). For the SAP model, food was withheld from age- and sex-matched littermates for 18 hours, but mice were provided water ad libitum. Moreover, mice received 8 hourly i.p. injections of saline (control) or of 50 g/kg cerulein (Sigma-Aldrich) in saline for 5 days.

Scores in AP and ALL. Histological analysis of pancreatitis and lung injury was performed as described previously (21). For evaluation of lung inflammation during pancreatitis, we randomly chose 10 microscopic fields per mouse (n = 4). Alveolar wall thickening was measured by 2 researchers in a blinded manner and analyzed using Axiovision software (version 4.8.; Zeiss).

Drug treatment in vivo. For inhibition experiments, sgp130Fc was provided by the Institute of Biochemistry, University of Kiel (endotoxin level, <0.125 EU/mg) and used according to the protocol in Supplemental Figure 5A. The small-molecule inhibitor S3I-201 (OTAVA) was freshly diluted from frozen aliquots in DMSO that had been stored at -20°C (stock concentration, 0.25 M). 9-week-old mice were injected i.v. with S3I-201 (7.5 mg/kg body weight) 2 hours after the first injection of cerulein. The CXCR2 antagonist SB225002 (2725; TORCIS Bioscience) was diluted in DMSO and injected i.p. at a concentration of 0.5 µg/g body weight. The anti-CXCL1 antibody (MAB4531; R&D Systems) was injected i.p. on days 1 and 3 of treatment (50 µg). Control mice were treated in parallel with respective concentrations of DMSO (0.082 µl/g) in PBS as a vehicle control. Animals were stratified, and the pancreases were analyzed.

Flow cytometry. Harvested lungs were injected with 1.0 mg/ml collagenase D (Roche) and 1.0 mg/ml DNase 1 (Sigma-Aldrich) and minced. Single-cell suspensions of lung cells were immunolabeled with fluorochrome-conjugated antibodies in PBS that were supplemented with 2% heat-inactivated FBS (Gibco, Invitrogen) and 5 mM EDTA (Sigma-Aldrich). All antibodies were purchased from eBioscience, including PE-conjugated antibody to Gr-1 (clone RB6-8C5) and APC-eFluor 780-conjugated CD11b-specific antibody (clone M1/70). Cells were stained with propidium iodide (BD

Biosciences) to assess viability. Flow cytometry analysis was performed on a Gallios flow cytometer (Beckman Coulter) after gating and excluding dead cells. Data were analyzed using FlowJo software.

Human samples. Patients with AP who were admitted to Scania University Hospital (Malmö, Sweden) were included in the study. AP was defined as upper abdominal pain and elevated serum amylase levels (minimum 3 times the upper reference limit) and/or radiological findings that confirmed AP. No patients were referred from other hospitals. Patients were considered to have SAP (n = 6) or mild pancreatitis (n = 20) based on the Atlanta criteria (51). Blood samples were placed in PST tubes and centrifuged (2,000 g, 25°C, 10 minutes), and plasma was frozen at -80°C.

Statistics. Data are presented as mean ± SD and were analyzed with a built-in 2-tailed t test using Microsoft Excel. A P value less than 0.05 was considered significant.

Study approval. All animal experiments were reviewed and approved by the Regierung von Oberbayern (reference no. 55.2-1-54-2531-189-09; Munich, Germany). The human study was approved by the regional research ethics committee at Lund University (approval no. 2009/413). Oral and written informed consent was provided by all patients before entrance into the study.

Acknowledgments

We thank Karen Dlubatz for excellent technical assistance, Georg Waetzig (Conaris Research Institute, Kiel, Germany) for help with preparing sgp130Fc, Andreas Blutke for help with blood pressure experiments, and Paul Ziegler for assisting with flow cytometry analysis. This work is a part of the doctoral thesis of P. Neuhöfer. H. Zhang was supported as a guest scientist by Sonderforschungsbereich 576 (Teilprojekt A 10). Y. Akihiko received grants from the Ministry of Education, Culture, Sports, Science, and Technology of Japan and the Program for Promotion of Fundamental Studies in Health Sciences of the National Institute of Biomedical Innovation. The work of S. Rose-John was supported by Deutsche Forschungsgemeinschaft (SFB841, TP C1) and the Cluster of Excellence – “Inflammation at Interfaces.” H. Algül and R.M. Schmid were supported by Deutsche Forschungsgemeinschaft (SFB576, TP A10; AL1174/3-1) and the Else Kröner Fresenius Stiftung (2010-A144).

Received for publication May 23, 2012, and accepted in revised form December 17, 2012.

Address correspondence to: Hana Algül, II. Medizinische Klinik, Klinikum rechts der Isar, Technische Universität München, 81675 Munich, Germany. Phone: 49.89.4140.5215; Fax: 49.89.4140.6794; E-mail: hana.alguel@lrz.tum.de.

1. Whitcomb DC. Clinical practice. Acute pancreatitis. *N Engl J Med.* 2006;354(20):2142–2150.
2. Bone RC. Sepsis, the sepsis syndrome, multi-organ failure: a plea for comparable definitions. *Ann Intern Med.* 1991;114(4):332–333.
3. Hotchkiss RS, Karl IE. The pathophysiology and treatment of sepsis. *N Engl J Med.* 2003;348(2):138–150.
4. Riedemann NC, Guo RF, Ward PA. Novel strategies for the treatment of sepsis. *Nat Med.* 2003;9(5):S17–S24.
5. Rinderknecht H. Fatal pancreatitis, a consequence of excessive leukocyte stimulation? *Int J Pancreatol.* 1988;3(2–3):105–112.
6. Paterson RL, Webster NR. Sepsis and the systemic inflammatory response syndrome. *J R Coll Surg Edinb.* 2000;45(3):178–182.
7. Muddana V, Whitcomb DC, Papachristou GI. Current management and novel insights in acute pancreatitis. *Expert Rev Gastroenterol Hepatol.* 2009;3(4):435–444.
8. Pezzilli R, Bellacosa L, Felicani C. Lung injury in acute pancreatitis. *JOP.* 2009;10(5):481–484.
9. Whitcomb DC, et al. Hereditary pancreatitis is caused by a mutation in the cationic trypsinogen gene. *Nat Genet.* 1996;14(2):141–145.
10. Witt H, et al. Mutations in the gene encoding the serine protease inhibitor, Kazal type 1 are associated with chronic pancreatitis. *Nat Genet.* 2000;25(2):213–216.
11. Papachristou GI. Prediction of severe acute pancreatitis: current knowledge and novel insights. *World J Gastroenterol.* 2008;14(41):6273–6275.
12. Leser HG, et al. Elevation of serum interleukin-6 concentration precedes acute-phase response and reflects severity in acute pancreatitis. *Gastroenterology.* 1991;101(3):782–785.
13. Viedma JA, Perez-Mateo M, Dominguez JE, Carballo F. Role of interleukin-6 in acute pancreatitis. Comparison with C-reactive protein and phospholipase A. *Gut.* 1992;33:1264–1267.
14. Arnaud C, et al. Statins reduce interleukin-6-induced C-reactive protein in human hepatocytes: new evidence for direct antiinflammatory effects of statins. *Arterioscler Thromb Vasc Biol.* 2005;25(6):1231–1236.
15. Jostock T, et al. Soluble gp130 is the natural inhibitor of soluble interleukin-6 receptor transsignaling responses. *Eur J Biochem.* 2001;268(1):160–167.
16. Jones SA, Richards PJ, Scheller J, Rose-John S. IL-6 transsignaling: the in vivo consequences. *J Interferon Cytokine Res.* 2005;25(5):241–253.
17. Rabe B, et al. Transgenic blockade of interleukin 6 transsignaling abrogates inflammation. *Blood.* 2008;111(3):1021–1028.
18. Reipschlag S, et al. Toxin-induced RhoA activity mediates CCL1-triggered signal transducers and activators of transcription protein signaling. *J Biol Chem.* 2012;287(14):11183–11194.
19. Birukova AA, Tian Y, Meliton A, Leff A, Wu T, Birukov KG. Stimulation of Rho signaling by pathologic mechanical stretch is a “second hit” to Rho-independent lung injury induced by IL-6. *Am J Physiol*



- Lung Cell Mol Physiol.* 2012;302(9):L965–L975.
20. Yu H, Pardoll D, Jove R. STATs in cancer inflammation and immunity: a leading role for STAT3. *Nat Rev Cancer.* 2009;9(11):798–809.
 21. Algul H, et al. Pancreas-specific RelA/p65 truncation increases susceptibility of acini to inflammation-associated cell death following cerulein pancreatitis. *J Clin Invest.* 2007;117(6):1490–1501.
 22. Ethridge RT, et al. Cyclooxygenase-2 gene disruption attenuates the severity of acute pancreatitis and pancreatitis-associated lung injury. *Gastroenterology.* 2002;123(4):1311–1322.
 23. Cuzzocrea S, et al. Absence of endogenous interleukin-6 enhances the inflammatory response during acute pancreatitis induced by cerulein in mice. *Cytokine.* 2002;18(5):274–285.
 24. Pandolfi SJ, Saluja AK, Imrie CW, Banks PA. Acute pancreatitis: bench to the bedside. *Gastroenterology.* 2007;132(3):1127–1151.
 25. Sander LE, et al. Hepatic acute-phase proteins control innate immune responses during infection by promoting myeloid-derived suppressor cell function. *J Exp Med.* 2010;207(7):1453–1464.
 26. Klein C, et al. The IL-6-gp130-STAT3 pathway in hepatocytes triggers liver protection in T cell-mediated liver injury. *J Clin Invest.* 2005;115(4):860–869.
 27. Fischer M, et al. I. A bioactive designer cytokine for human hematopoietic progenitor cell expansion. *Nat Biotechnol.* 1997;15(2):142–145.
 28. Sun R, Jaruga B, Kulkarni S, Sun H, Gao B. IL-6 modulates hepatocyte proliferation via induction of HGF/p21cip1: regulation by SOCS3. *Biochem Biophys Res Commun.* 2005;338(4):1943–1949.
 29. Chalaris A, et al. Apoptosis is a natural stimulus of IL6R shedding and contributes to the proinflammatory trans-signaling function of neutrophils. *Blood.* 2007;110(6):1748–1755.
 30. Atreya R, et al. Blockade of interleukin 6 trans-signaling suppresses T-cell resistance against apoptosis in chronic intestinal inflammation: evidence in crohn disease and experimental colitis in vivo. *Nat Med.* 2000;6(5):583–588.
 31. Jones SA, Scheller J, Rose-John S. Therapeutic strategies for the clinical blockade of IL-6/gp130 signaling. *J Clin Invest.* 2011;121(9):3375–3383.
 32. Szczepanek K, Lesnefsky EJ, Larner AC. Multitasking: nuclear transcription factors with novel roles in the mitochondria. *Trends Cell Biol.* 2012;22(8):429–437.
 33. Neuhöfer P, et al. Deletion of IkappaBalpha activates RelA to reduce acute pancreatitis in mice through upregulation of Spi2A. *Gastroenterology.* 2013;144(1):192–201.
 34. Lesina M, et al. Stat3/Socs3 activation by IL-6 transsignaling promotes progression of pancreatic intraepithelial neoplasia and development of pancreatic cancer. *Cancer Cell.* 2011;19(4):456–469.
 35. Siddiquee K, et al. Selective chemical probe inhibitor of Stat3, identified through structure-based virtual screening, induces antitumor activity. *Proc Natl Acad Sci U S A.* 2007;104(18):7391–7396.
 36. Inagaki T, et al. Interleukin-6 is a useful marker for early prediction of the severity of acute pancreatitis. *Pancreas.* 1997;14(1):1–8.
 37. von Bismarck P, Claass A, Schickor C, Krause MF, Rose-John S. Altered pulmonary interleukin-6 signaling in preterm infants developing bronchopulmonary dysplasia. *Exp Lung Res.* 2008;34(10):694–706.
 38. Malmström ML, et al. Cytokines and organ failure in acute pancreatitis: inflammatory response in acute pancreatitis. *Pancreas.* 2012;41(2):271–277.
 39. Lin WC, Lin CF, Chen CL, Chen CW, Lin YS. Prediction of outcome in patients with acute respiratory distress syndrome by bronchoalveolar lavage inflammatory mediators. *Exp Biol Med (Maywood).* 2010;235(1):57–65.
 40. Chao KC, Chao KF, Chuang CC, Liu SH. Blockade of interleukin 6 accelerates acinar cell apoptosis and attenuates experimental acute pancreatitis in vivo. *Br J Surg.* 2006;93(3):332–338.
 41. Scheller J, Chalaris A, Schmidt-Arras D, Rose-John S. The pro- and anti-inflammatory properties of the cytokine interleukin-6. *Biochim Biophys Acta.* 2011;1813(5):878–888.
 42. Linker RA, et al. IL-6 transsignaling modulates the early effector phase of EAE and targets the blood-brain barrier. *J Neuroimmunol.* 2008;205(1–2):64–72.
 43. Regner S, Appelros S, Hjalmarsson C, Manjer J, Sadic J, Borgstrom A. Monocyte chemoattractant protein 1, active carboxypeptidase B and CAPAP at hospital admission are predictive markers for severe acute pancreatitis. *Pancreatology.* 2008;8(1):42–49.
 44. Quinton LJ, et al. Hepatocyte-specific mutation of both NF-κB RelA and STAT3 abrogates the acute phase response in mice. *J Clin Invest.* 2012;122(5):1758–1763.
 45. Konrad FM, Reutershan J. CXCR2 in acute lung injury. *Mediators Inflamm.* 2012;2012:740987.
 46. Park WY, et al. Cytokine balance in the lungs of patients with acute respiratory distress syndrome. *Am J Respir Crit Care Med.* 2001;164(10 pt 1):1896–1903.
 47. Barkhausen T, et al. Selective blockade of interleukin-6 trans-signaling improves survival in a murine polymicrobial sepsis model. *Crit Care Med.* 2011;39(6):1407–1413.
 48. Matthay MA, Zemans RL. The acute respiratory distress syndrome: pathogenesis and treatment. *Annu Rev Pathol.* 2011;6:147–163.
 49. Waetzig GH, Rose-John S. Hitting a complex target: an update on interleukin-6 trans-signaling. *Expert Opin Ther Targets.* 2012;16(2):225–236.
 50. Herbert DR, et al. Alternative macrophage activation is essential for survival during schistosomiasis and downmodulates T helper 1 responses and immunopathology. *Immunity.* 2004;20(5):623–635.
 51. Bradley EL 3rd. A clinically based classification system for acute pancreatitis. Summary of the International Symposium on Acute Pancreatitis, Atlanta, Ga, September 11 through 13, 1992. *Arch Surg.* 1993;128(5):586–590.